Identification of the Stress-Strain State of a Cylindrical Tank with Walls of Variable Thickness

Mirko Đelošević
Researcher
University of Kragujevac
Faculty of Mechanical Engineering, Kraljevo

Dragan Petrović
Associate Professor
University of Kragujevac
Faculty of Mechanical Engineering, Kraljevo

Milan Bižić
Assistant
University of Kragujevac
Faculty of Mechanical Engineering, Kraljevo

This paper presents the stress-strain analysis of a cylindrical tank shell made of two segments with different thickness, loaded by the hydrostatic pressure of water. Physical and mathematical models relevant for the analysis of deflection and stresses of the tank shell as a function of hydrostatic pressure are built. Functions of distribution of deflection, transverse forces and appropriate moments of the tank shell, i.e. tank segments, as well as stresses are determined. The mutual influences among the tank segments, depending on the length and thickness of the plate of applied segments, are identified, which creates the possibilty of optimum design of tanks that are symmetrically loaded in relation to the axis. The results obtained by the analytical procedure correspond to the results of FEM. Diagrams of distribution of deflection, moments, transverse forces and stresses are identical, while the maximum deviation of those values does not exceed 5 %.

Keywords: *shell, tank, strain, stress, pressure.*

1. INTRODUCTION

This paper presents the identification of the stress-strain state of a cylindrical tank by the application of the general theory of cylindrical shells, i.e. theory of cylindrical shells loaded symmetrically in relation to the axis. The subject of the analysis is a cylindrical tank composed of two segments, heights h_1 and h_2, i.e. thicknesses δ_1 and δ_2 (Fig. 1). The methodology applied in this example does not reduce the generality of application in the tanks composed of several segments made of plates with different thicknesses. Namely, the conditions that hold in the section of joint between two segments (section “A-A”, according to Figure 1) are identical to the conditions, when there are several segments (e.g. 4, in sections “B-B”, “C-C” and “D-D”, according to Figure 2). That is why the analysis of the tank from Figure 1 will be carried out in the further procedure.

Also, the analysis procedure is based on accurate expressions, which is very important in the cases when the thickness of tank segment walls cannot be neglected in relation to the height and diameter. Then the application of expressions which hold for an infinitely long tank according to [1] is not sufficiently correct, and hence it is necessary to consider the mutual influences among certain segments of the observed tank. The theoretical postulates of the mentioned analysis are given in [1-3]. The tanks made of segments with different thicknesses and loaded by hydrostatic pressure are frequently used in practice because of the rational exploitation of material. The segments that are exposed to higher hydrostatic pressure are made of thick plates (segments closer to the tank bottom), while thin plates are used for the other segments (closer to the top of the tank), due to lower pressure. The subject of stress-strain identification is primarily the tank shell, while the bottom is supposed to be supported by a sufficient surface, so that there are no significant deformations, i.e. the influence of the bottom on the tank shell is negligible in relation to the load by hydrostatic pressure. Recent research into cylindrical shells [4-7] shows modern approaches in the analysis of stress state based on FEM and experimental testing. In this paper, the methodology of stress-strain identification of cylindrical shells, within the mentioned research, points out the effect of rational exploitation of material. The fact that utilization of shells with variable thickness has favourable influences on the phenomenon of local stress is of particular importance. Stresses at critical points of the tank can be reduced by inserting reinforcements (ring), but the consequence would be a negative effect of local stress in their neighbourhood, which was in detail analysed in research [2].

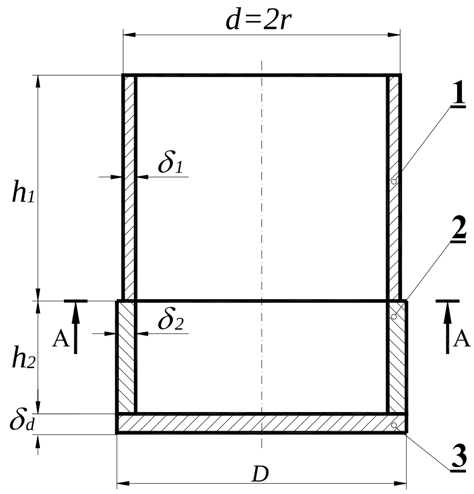

Figure 1. Cylindrical tank with two segments

Received: November 2010, Accepted: February 2011
Correspondence to: Mirko Đelošević
Faculty of Mechanical Engineering,
Dositejeva 19, 36000 Kraljevo, Serbia
E-mail: djelosevic.m@mfkv.kg.ac.rs

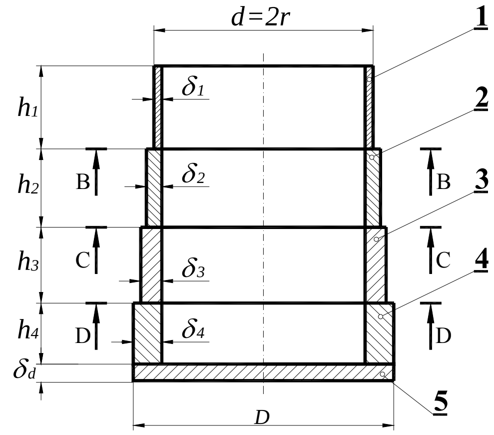

Figure 2. Cylindrical tank with four segments

2. METHODOLOGY OF THE THEORETICAL ANALYSIS

Mathematical modelling of the cylindrical tank shell will be performed in the example given in Figure 3. As the tank shell consists of two segments (pos. 1 and 2), besides the fixed-end reactions (Q_0 and M_0), there are internal reactions in the contact between two segments (Q_1 and M_1), according to Figure 4.

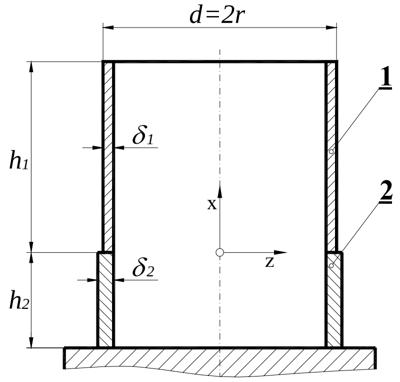

Figure 3. Model of the cylindrical tank with two segments

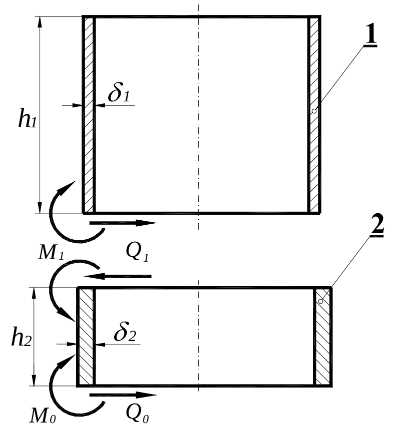

Figure 4. Internal and external reactions of two segments

The differential equation of the elastic surface of the cylindrical shell symmetrically loaded in relation to the axis, according to [1-3], is:

$$\frac{\mathrm{d}^4 w}{\mathrm{d}x^4} + 4\beta^4 w = \frac{Z}{D} \tag{1}$$

where the coefficient determined according to (2):

$$\beta^4 = \frac{E\delta}{4r^2 D} = \frac{3(1-\nu^2)}{r^2\delta^2} \tag{2}$$

where the flexural rigidity of the shell:

$$D = \frac{E\delta^3}{12(1-\nu^2)} . \tag{3}$$

The deflection of the round cylindrical shell, symmetrically loaded in relation to the axis, is given by the expression:

$$w = e^{\beta x}\left[C_1 \cos(\beta x) + C_2 \sin(\beta x)\right] +$$

$$+ e^{-\beta x}\left[C_3 \cos(\beta x) + C_4 \sin(\beta x)\right] + w_p(x) . \tag{4}$$

The particular solution will be assumed in the form:

$$w_p(x) = Ax + B . \tag{5}$$

A and B are indefinite coefficients, which are obtained according to (6) and (7) by substituting (4) in (1), we obtain:

$$4\beta^4 (Ax + B) = -\frac{\rho g (h_1 - x)}{D} \tag{6}$$

$$(4\beta^4 A)x = \frac{\rho g}{D} x \Rightarrow A = \frac{\rho g}{4\beta^4 D} \tag{7}$$

$$4\beta^4 B = -\frac{\rho g h_1}{D} \Rightarrow B = -\frac{\rho g h_1}{4\beta^4 D} . \tag{8}$$

The particular load (w_p) which corresponds to the load by hydrostatic pressure (Z) has the form:

$$w_p = -\frac{\rho g (h_1 - x)}{4\beta^4 D} = -\frac{\rho g (h_1 - x)}{E\delta} r^2 . \tag{9}$$

The general solution of (1) has the form:

$$w(x) = e^{\beta x}\left[C_1 \cos(\beta x) + C_2 \sin(\beta x)\right] +$$

$$+ e^{-\beta x}\left[C_3 \cos(\beta x) + C_4 \sin(\beta x)\right] - \frac{\rho g (h_1 - x)}{E\delta} r^2 . \tag{10}$$

Since the tank is composed of two segments, with different stiffnesses, it is necessary to form two different distributions of the elastic surface in each tank segment.

On the basis of that, we have:

- for: $0 \le x \le h_1$

$$w_1(x) = e^{\beta_1 x}\left[C_1 \cos(\beta x) + C_2 \sin(\beta x)\right] +$$

$$+ e^{-\beta_1 x}\left[C_3 \cos(\beta x) + C_4 \sin(\beta x)\right] - \frac{\rho g (h_1 - x)}{E\delta_1} r^2 \tag{11}$$

i.e.

- for: $-h_2 \le x \le 0$

$$w_2(x) = e^{\beta_2 x}\left[C_5 \cos(\beta x) + C_6 \sin(\beta x)\right] +$$

$$+ e^{-\beta_2 x}\left[C_7 \cos(\beta x) + C_8 \sin(\beta x)\right] - \frac{\rho g (h_1 - x)}{E\delta_2} r^2 . \tag{12}$$

The constants of integration (C_1, C_2, ... C_8) are determined from the contour conditions at the ends of the tank (for $x = h_1$ and $x = -h_2$), as well as in the section of joint between two segments of the tank (section "A-A", for $x = 0$, according to Figure 1).

The contour conditions are:

$$(M_x)_{x=h_1} = -D_1 \left(\frac{\mathrm{d}^2 w_1}{\mathrm{d}x^2} \right)_{x=h_1} = 0 \quad (13)$$

$$(Q_x)_{x=h_1} = -D_1 \left(\frac{\mathrm{d}^3 w_1}{\mathrm{d}x^3} \right)_{x=h_1} = 0 \quad (14)$$

$$(w_1)_{x=0} = (w_2)_{x=0} \quad (15)$$

$$\left(\frac{\mathrm{d}w_1}{\mathrm{d}x} \right)_{x=0} = \left(\frac{\mathrm{d}w_2}{\mathrm{d}x} \right)_{x=0} \quad (16)$$

$$-D_1 \left(\frac{\mathrm{d}^2 w_1}{\mathrm{d}x^2} \right)_{x=0} = -D_2 \left(\frac{\mathrm{d}^2 w_2}{\mathrm{d}x^2} \right)_{x=0} \quad (17)$$

$$-D_1 \left(\frac{\mathrm{d}^3 w_1}{\mathrm{d}x^3} \right)_{x=0} = -D_2 \left(\frac{\mathrm{d}^3 w_2}{\mathrm{d}x^3} \right)_{x=0} \quad (18)$$

$$(w_2)_{x=-h_2} = 0 \quad (19)$$

$$\left(\frac{\mathrm{d}w_2}{\mathrm{d}x} \right)_{x=-h_2} = 0 \,. \quad (20)$$

The tank from Figure 3 is loaded by hydrostatic pressure of water, i.e. we have:

$$Z = -\rho g (h_1 - x) \,. \quad (21)$$

The tank dimensions relevant for calculation are as follows: $r = 4625$ mm; $h_1 = 7200$ mm; $h_2 = 3600$ mm; $\delta_1 = 6.0$ mm; $\delta_2 = 7.8$ mm.

The coefficients β_1 and β_2 are determined according to:

$$\beta_1^4 = \frac{3(1-\nu^2)}{r^2 \delta_1^2}, \text{ i.e. } \beta_2^4 = \frac{3(1-\nu^2)}{r^2 \delta_2^2} \,. \quad (22)$$

The derivatives of the function

$$w(x) = e^{\beta x} \left[C_1 \cos(\beta x) + C_2 \sin(\beta x) \right] + \\ + e^{-\beta x} \left[C_3 \cos(\beta x) + C_4 \sin(\beta x) \right] - \frac{\rho g (h_1 - x)}{E \delta} r^2 \quad (23)$$

are:

$$\frac{\mathrm{d}w}{\mathrm{d}x} = \beta e^{\beta x} \left[(-C_1 + C_2) \sin(\beta x) + (C_1 + C_2) \cos(\beta x) \right] + \\ + \beta e^{-\beta x} \left[(-C_3 - C_4) \sin(\beta x) + (-C_3 + C_4) \cos(\beta x) \right] + \\ + \frac{\rho g r^2}{E \delta} \quad (24)$$

$$\frac{\mathrm{d}^2 w}{\mathrm{d}x^2} = 2\beta^2 e^{\beta x} \left[-C_1 \sin(\beta x) + C_2 \cos(\beta x) \right] + \\ + 2\beta e^{-\beta x} \left[C_3 \sin(\beta x) - C_4 \cos(\beta x) \right] \quad (25)$$

$$\frac{\mathrm{d}^3 w}{\mathrm{d}x^3} = 2\beta^3 e^{\beta x} \left[(-C_1 - C_2) \sin(\beta x) + (-C_1 + C_2) \cos(\beta x) \right] + \\ + 2\beta^3 e^{-\beta x} \left[(-C_3 + C_4) \sin(\beta x) + (C_3 + C_4) \cos(\beta x) \right] . \quad (26)$$

When the function $w_1(x)$ is used, then there are the coefficients: C_1, C_2, C_3 and C_4.

When the function $w_2(x)$ is used, then there are the coefficients: C_5, C_6, C_7 and C_8.

Substituting (20) to (25) in (12) to (19), taking care that (10) holds on segment "1", i.e. (11) on segment "2", we obtain:

$$C_1 \left\{ -e^{\beta_1 h_1} \sin(\beta_1 h_1) \right\} + C_2 \left\{ e^{\beta_1 h_1} \cos(\beta_1 h_1) \right\} + C_3 \left\{ e^{-\beta_1 h_1} \sin(\beta_1 h_1) \right\} + C_4 \left\{ -e^{-\beta_1 h_1} \cos(\beta_1 h_1) \right\} = 0 \quad (27)$$

$$C_1 \left\{ -e^{\beta_1 h_1} \left[\sin(\beta_1 h_1) + \cos(\beta_1 h_1) \right] \right\} + C_2 \left\{ e^{\beta_1 h_1} \left[\cos(\beta_1 h_1) - \sin(\beta_1 h_1) \right] \right\} + \\ C_3 \left\{ e^{-\beta_1 h_1} \left[\cos(\beta_1 h_1) - \sin(\beta_1 h_1) \right] \right\} + C_4 \left\{ e^{-\beta_1 h_1} \left[\sin(\beta_1 h_1) + \cos(\beta_1 h_1) \right] \right\} = 0 \quad (28)$$

$$C_1 + C_3 - C_5 - C_7 = \frac{\rho g h_1 r^2}{E} \left[\frac{1}{\delta_1} - \frac{1}{\delta_2} \right] \quad (29)$$

$$C_1 \{\beta_1\} + C_2 \{\beta_1\} + C_3 \{-\beta_1\} + C_4 \{\beta_1\} + C_5 \{-\beta_2\} + C_6 \{-\beta_2\} + C_7 \{\beta_2\} + C_8 \{-\beta_2\} = -\frac{\rho g r^2}{E} \left[\frac{1}{\delta_1} - \frac{1}{\delta_2} \right] \quad (30)$$

$$C_2 \left\{ 2\beta_1^2 \right\} + C_4 \left\{ -2\beta_1^2 \right\} + C_6 \left\{ -2\frac{\delta_2}{\delta_1} \beta_2^2 \right\} + C_8 \left\{ 2\frac{\delta_2}{\delta_1} \beta_2^2 \right\} = 0 \quad (31)$$

$$C_1 \left\{ -2\beta_1^3 \right\} + C_2 \left\{ 2\beta_1^3 \right\} + C_3 \left\{ 2\beta_1^3 \right\} + C_4 \left\{ 2\beta_1^3 \right\} + C_5 \left\{ 2\frac{\delta_2}{\delta_1} \beta_2^3 \right\} + C_6 \left\{ -2\frac{\delta_2}{\delta_1} \beta_2^3 \right\} + C_7 \left\{ -2\frac{\delta_2}{\delta_1} \beta_2^3 \right\} + C_8 \left\{ -2\frac{\delta_2}{\delta_1} \beta_2^3 \right\} = 0 \quad (32)$$

$$C_5 \left\{ -e^{-\beta_2 h_2} \cos(-\beta_2 h_2) \right\} + C_6 \left\{ e^{-\beta_2 h_2} \sin(-\beta_2 h_2) \right\} + C_7 \left\{ e^{\beta_2 h_2} \cos(-\beta_2 h_2) \right\} + C_8 \left\{ e^{\beta_2 h_2} \sin(-\beta_2 h_2) \right\} = \frac{\rho g h r^2}{E \delta_2} \quad (33)$$

$$C_5\left\{\beta_2 e^{-\beta_2 h_2}\left[\cos(-\beta_2 h_2)-\sin(-\beta_2 h_2)\right]\right\}+C_6\left\{\beta_2 e^{-\beta_2 h_2}\left[\sin(-\beta_2 h_2)+\cos(-\beta_2 h_2)\right]\right\}+$$

$$C_7\left\{\beta_2 e^{\beta_2 h_2}\left[\sin(-\beta_2 h_2)+\cos(-\beta_2 h_2)\right]\right\}+C_8\left\{\beta_2 e^{\beta_2 h_2}\left[\cos(-\beta_2 h_2)-\sin(-\beta_2 h_2)\right]\right\}=\frac{\rho g r^2}{E\delta_2}. \quad (34)$$

The previous system of algebraic equations can be written in the matrix form:

$$\{C_i\}\cdot[K]=\{Q\}. \quad (35)$$

The column matrix $\{C_i\}$ is determined on the basis of the matrix equation:

$$\{C_i\}=[K]^{-1}\cdot\{Q\} \quad (36)$$

where:

$$\{C_i\}=\{C_1 \quad C_2 \quad C_3 \quad C_4 \quad C_5 \quad C_6 \quad C_7 \quad C_8\}^T \quad (37)$$

$$[K]=\begin{bmatrix} k_1 & k_2 & k_3 & k_4 & 0 & 0 & 0 & 0 \\ k_5 & k_6 & k_7 & k_8 & 0 & 0 & 0 & 0 \\ 1 & 0 & 1 & 0 & -1 & 0 & -1 & 0 \\ k_9 & k_9 & -k_9 & k_9 & -k_{10} & -k_{10} & k_{10} & -k_{10} \\ 0 & k_{11} & 0 & -k_{11} & 0 & -k_{12} & 0 & k_{12} \\ -k_{13} & k_{13} & k_{13} & k_{13} & k_{14} & -k_{14} & -k_{14} & -k_{14} \\ 0 & 0 & 0 & 0 & k_{15} & k_{16} & k_{17} & k_{18} \\ 0 & 0 & 0 & 0 & k_{19} & k_{20} & k_{21} & k_{22} \end{bmatrix} \quad (38)$$

$$\{Q\}=\begin{Bmatrix} 0 \\ 0 \\ \dfrac{\rho g h_1 r^2}{E}\left[\dfrac{1}{\delta_1}-\dfrac{1}{\delta_2}\right] \\ -\dfrac{\rho g r^2}{E}\left[\dfrac{1}{\delta_1}-\dfrac{1}{\delta_2}\right] \\ 0 \\ 0 \\ \dfrac{\rho g h r^2}{E\delta_2} \\ -\dfrac{\rho g r^2}{E\delta_2} \end{Bmatrix}. \quad (39)$$

The matrix coefficients (37) are given in Table 1.

By solving (35), we obtain the required coefficients:

$$\begin{Bmatrix} C_1 \\ C_2 \\ C_3 \\ C_4 \\ C_5 \\ C_6 \\ C_7 \\ C_8 \end{Bmatrix}=\begin{Bmatrix} 0 \\ 0 \\ 1.331\cdot 10^{-4} \\ -1.352\cdot 10^{-6} \\ -1.489\cdot 10^{-4} \\ 1.352\cdot 10^{-6} \\ 1.198\cdot 10^{-15} \\ 5.197\cdot 10^{-14} \end{Bmatrix}\left(\frac{1}{m}\right). \quad (40)$$

On the basis of the values of these coefficients, the diagrams of distribution of deflections $w_1(x)$ and $w_2(x)$ can be formed.

Table 1. Coefficients of introduced replacements

k_1	$-e^{\beta_1 h_1}\sin(\beta_1 h_1)$
k_2	$e^{\beta_1 h_1}\cos(\beta_1 h_1)$
k_3	$e^{-\beta_1 h_1}\sin(\beta_1 h_1)$
k_4	$-e^{-\beta_1 h_1}\cos(\beta_1 h_1)$
k_5	$-e^{\beta_1 h_1}\left[\sin(\beta_1 h_1)+\cos(\beta_1 h_1)\right]$
k_6	$e^{\beta_1 h_1}\left[\cos(\beta_1 h_1)-\sin(\beta_1 h_1)\right]$
k_7	$e^{-\beta_1 h_1}\left[\cos(\beta_1 h_1)-\sin(\beta_1 h_1)\right]$
k_8	$e^{-\beta_1 h_1}\left[\sin(\beta_1 h_1)+\cos(\beta_1 h_1)\right]$
k_9	β_1
k_{10}	β_2
k_{11}	$2\beta_1^2$
k_{12}	$2(\delta_2/\delta_1)\beta_2^2$
k_{13}	$2\beta_1^3$
k_{14}	$2(\delta_2/\delta_1)\beta_2^3$
k_{15}	$-e^{-\beta_2 h_2}\cos(-\beta_2 h_2)$
k_{16}	$e^{-\beta_2 h_2}\sin(-\beta_2 h_2)$
k_{17}	$e^{\beta_2 h_2}\cos(-\beta_2 h_2)$
k_{18}	$e^{\beta_2 h_2}\sin(-\beta_2 h_2)$
k_{19}	$\beta_2 e^{-\beta_2 h_2}\left[\cos(-\beta_2 h_2)-\sin(-\beta_2 h_2)\right]$
k_{20}	$\beta_2 e^{-\beta_2 h_2}\left[\sin(-\beta_2 h_2)+\cos(-\beta_2 h_2)\right]$
k_{21}	$\beta_2 e^{\beta_2 h_2}\left[\sin(-\beta_2 h_2)+\cos(-\beta_2 h_2)\right]$
k_{22}	$\beta_2 e^{\beta_2 h_2}\left[\cos(-\beta_2 h_2)-\sin(-\beta_2 h_2)\right]$

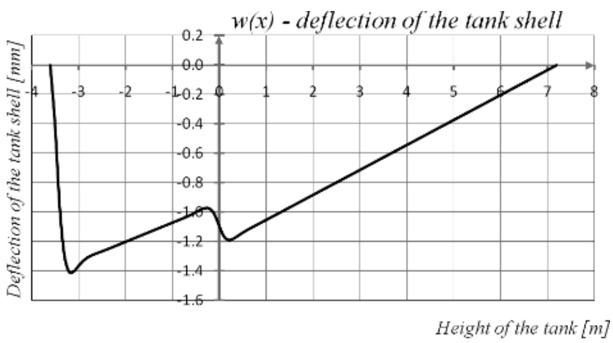

Figure 5. Diagram of distribution of deflections of the tank shell

The moment of the cylindrical shell of the tank is determined from the expression:

$$M_x = -D\left(\frac{\partial^2 w}{\partial x^2}\right). \tag{41}$$

The transverse force of the cylindrical shell of the tank is determined from the expression:

$$Q_x = -D\left(\frac{\partial^3 w}{\partial x^3}\right). \tag{42}$$

The moment in the circular direction (M_φ) is:

$$M_\varphi = \nu M_x . \tag{43}$$

The moment for segment “1” of the tank is:

$$\begin{aligned}(M_x)_1 &= -D_1\left(\frac{\partial^2 w_1}{\partial x^2}\right) = \\ &= -2D_1\beta_1^2\left\{e^{\beta_1 x}\left[-C_1\sin(\beta_1 x)+C_2\cos(\beta_1 x)\right]+\right. \\ &\left.+e^{-\beta_1 x}\left[C_3\sin(\beta_1 x)-C_4\cos(\beta_1 x)\right]\right\}. \end{aligned} \tag{44}$$

The transverse force for segment “1” of the tank is:

$$\begin{aligned}(Q_x)_1 &= -2D_1\beta_1^3\left\{e^{\beta_1 x}\left[(-C_1-C_2)\sin(\beta_1 x)+\right.\right. \\ &+(-C_1+C_2)\cos(\beta_1 x)\left.\right]+e^{-\beta_1 x}\left[(-C_3+C_4)\sin(\beta_1 x)+\right. \\ &\left.\left.+(C_3+C_4)\cos(\beta_1 x)\right]\right\}. \end{aligned} \tag{45}$$

The moment for segment “2” of the tank is:

$$\begin{aligned}(M_x)_2 &= -D_2\left(\frac{\partial^2 w_2}{\partial x^2}\right) = \\ &= -2D_2\beta_2^2\left\{e^{\beta_2 x}\left[-C_5\sin(\beta_2 x)+C_6\cos(\beta_2 x)\right]+\right. \\ &\left.+e^{-\beta_2 x}\left[C_7\sin(\beta_2 x)-C_8\cos(\beta_2 x)\right]\right\}. \end{aligned} \tag{46}$$

The transverse force for segment “2” of the tank is:

$$\begin{aligned}(Q_x)_2 &= -2D_2\beta_2^3\left\{e^{\beta_2 x}\left[(-C_5-C_6)\sin(\beta_2 x)+\right.\right. \\ &+(-C_5+C_6)\cos(\beta_2 x)\left.\right]+e^{-\beta_2 x}\left[(-C_7+C_8)\sin(\beta_2 x)+\right. \\ &\left.\left.+(C_7+C_8)\cos(\beta_2 x)\right]\right\}. \end{aligned} \tag{47}$$

The diagrams of distribution of moments, transverse forces and stresses are given in Figures 6, 7 and 8, respectively.

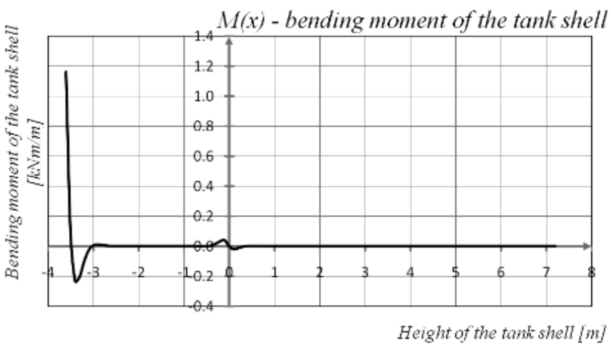

Figure 6. Diagram of distribution of the bending moment (M_x) of the tank shell

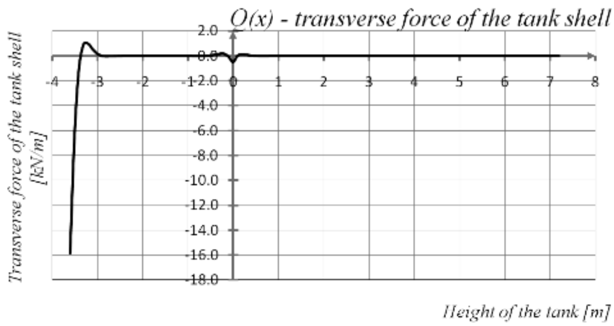

Figure 7. Diagram of distribution of the transverse force (Q_x) of the tank shell

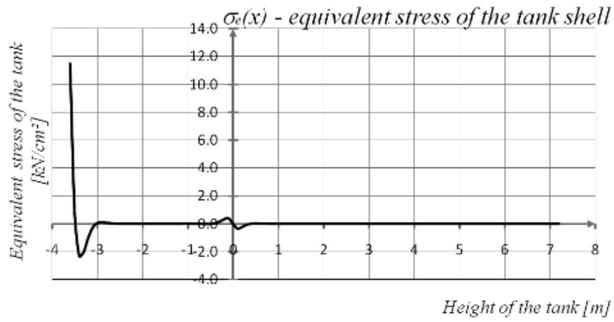

Figure 8. Diagram of distribution of the equivalent stress (σ_e) of the tank shell

Equivalent stress (Fig. 8), is:

$$\sigma_e = \sqrt{\sigma_x^2 + \sigma_\varphi^2 - \sigma_x\sigma_\varphi + 3\tau_{max}^2} < \sigma_{doz} . \tag{48}$$

For $\frac{\delta}{r} << 1$:

$$\sigma_x = \frac{6M_x}{\delta^2}; \; \sigma_\varphi = \frac{6M_\varphi}{\delta^2}; \; \tau_{max} = \frac{3Q_x}{2\delta} . \tag{49}$$

The importance of analytical methods in stress identification, especially in highly stressed tanks [8], is evident primarily in establishing correlations between certain parameters of the tank (e.g. between the lengths and heights of tank segments, depending on the pressure). The knowledge of such regularities is significant for determination of the stress-strain state, particularly in the zones of change of section, such as the transition from the spherical into the elliptical shape [9,10], but also for the optimum design of tanks [11]. In addition to analytical identifications of tank stress, there are significant results obtained by using FEM, [12-18]. A lot of engineering problems are solved by using this method. However, it is not suitable for the optimisation process, because it requires a large number of iterations, which extends the design period. The key activity in the application of FEM is the generation of a finite element mesh, and the triangle mesh [19] is most suitable for cylindrical shells.

3. RESULTS OBTAINED BY FEM

By using ANSYS software, which is based on FEM, the analysis of stress and strain, i.e. the analysis of deflection of the tank shell was carried out for the purpose of verifying the applied theory and the performed methodology of the identification considered.

The subject of analysis by applying FEM is the tank shell composed of 2 segments of different thicknesses. The value of hydrostatic pressure of water to which the tank shell is exposed as well as its dimensions are identical to the values used in the theoretical analysis, while the connection between the tank shell and the base is represented by fixed-end reactions. The FEM model is thus, with respect to load, geometry and constraints, identical to the theoretical model. The tetrahedral finite elements, size 22 mm, were applied for generation of the FEM model. Software calculation of the stress-strain state was performed on the basis of the model created, while the values read are presented in comparative diagrams of deflection and equivalent stress (Figs. 11 and 12). The trends of distribution of deflection and comparative stress, obtained by means of FEM, are in accordance with the trends of the same distributions calculated by the analytical procedure.

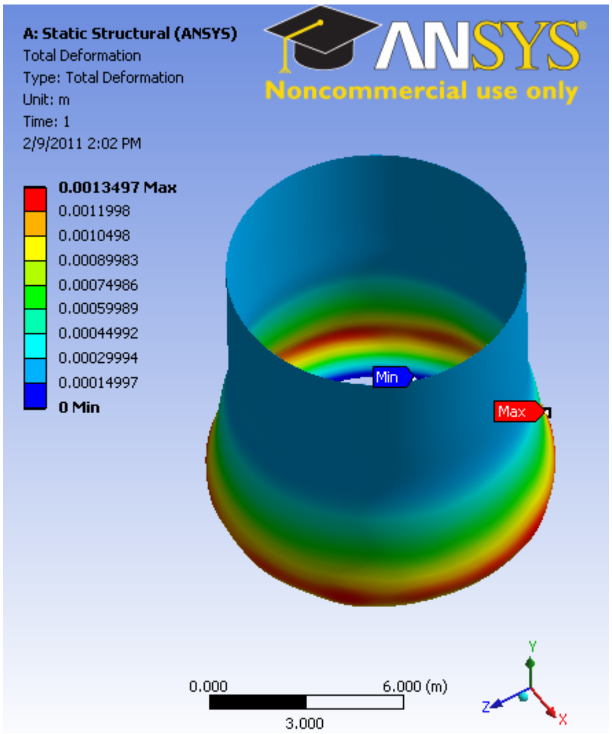

Figure 9. Total deformation tank of the shall (ANSYS)

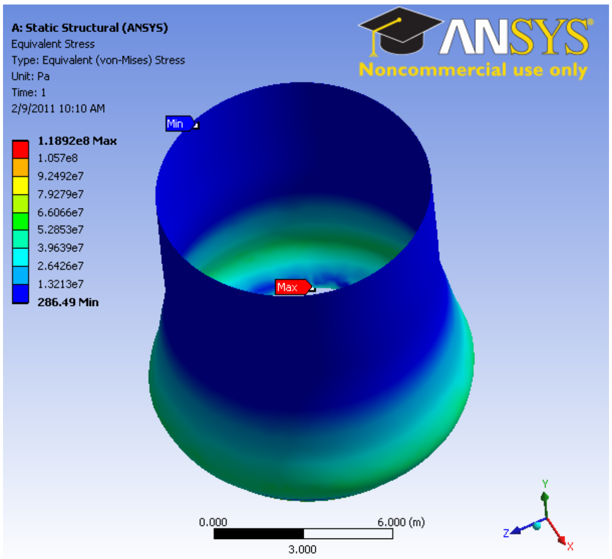

Figure 10. Equivalent stress (σ_e)

The FEM results for deflection and equivalent stress are presented in Figures 9 and 10, respectively.

3.1 Comparative analysis of the calculation procedure and the finite element method

By using the diagrams presented in Figures 11 and 12, the comparative analysis for the tank loaded by hydrostatic action of water, shown in Figure 1, can be carried out. The key values that are the subject of comparison are the deflection $w(x)$ and the bending stress $\sigma(x)$ of the tank shell.

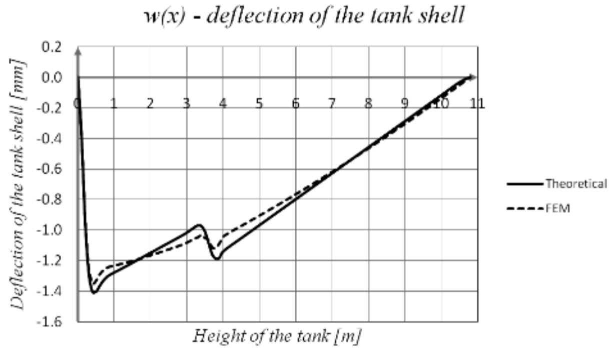

Figure 11. Diagram of deflections of the tank shell obtained by FEM

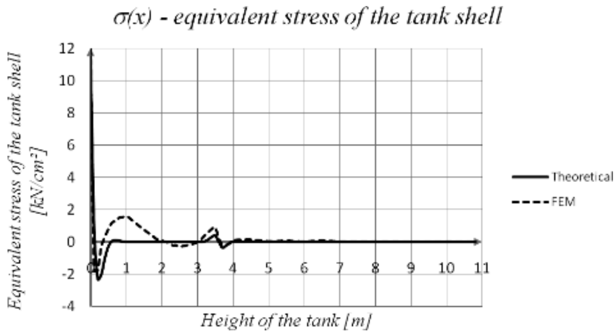

Figure 12. Diagram of distribution of equivalent stress of the tank shell obtained by the application of FEM

Table 2. Comparative analysis of the value

Name of the value	Analytical procedure (max. value)	FEM (max. value)	Deviation [%]
Shell deflection $w(x)$ [mm]	1.41	1.35	4.2
Equivalent stress $\sigma_e(x)$ [kN/cm^2]	11.46	11.89	3.6

4. FINAL CONSIDERATIONS

The previous presentation shows the analysis of the stress-strain state of the tank with two segments, where, on the basis of the diagram of the equivalent stress (Fig. 12), it can clearly be established that there is insufficiently rational exploitation of the material for the given dimensions of the tank. Therefore, in the considered case we should tend towards the increase in the number of segments in order to have the optimum tank structure. The increase in the number of segments for the constant height of the tank results in a more uniform distribution of the equivalent stress σ_x (without larger oscillation, i.e. peaks). It provides more rational exploitation of the material inserted. Also, the influence of the tank bottom on the stress-strain state of the tank shell is not taken into account and such an analysis gives results on the side of safety. Namely, if a certain deformation of the tank bottom were allowed, then it would be transferred to the shell through the corresponding moments, and the deformation would be smaller than in the case considered. By analyzing the stress diagram (Fig. 12), three characteristic zones of the tank shell can be established, i.e.:

1. The zone of joining between two segments (section "A-A", according to Figure 1);
2. The zone immediately before joining with the tank bottom (according to the case considered, it is the zone around the value $x = -3.4$ m);
3. The zone of joining between the tank shell and the tank bottom ($x = -3.6$ m), where the maximum value of stress occurs.

In the example considered, with two segments, there is a very uneven distribution of stresses, with pronounced peaks, and hence such a solution cannot be regarded as economical. The aspect for its improvement is seen in the increase of the number of segments (e.g. 4, according to Figure 2), so that segment no. 4 would have the role of elimination of the peak with the value 11.464 (kN/cm^2), and segment no. 3 would eliminate the value – 2.416 (kN/cm^2). Selection of plate thickness of certain segments defines the bending stress as well as the mutual influence between the segments. The optimum dimensions of the tank imply that the equivalent stress σ_x (Fig. 12) has a relatively uniform shape (close to the rectilinear line, without significant peaks) and the value immediately below the allowed stress (σ_{doz}).

Generally, the methodology used in tanks with two segments can be successfully applied to tanks with several segments, which is especially significant in design of tanks with large overall dimensions, where the techno-economic aspect cannot be neglected. Thus the condition for optimum design of the tank is provided.

REFERENCES

[1] Timoshenko, S. and Woinowsky-Krieger, S.: *Theory of Plates and Shells*, McGraw-Hill Book Company, New York, 1959.

[2] Ogibalov, P. and Anđelić, T.: *Mechanics of Shells and Plates*, Izdavačko informativni centar studenata, Belgrade, 1975, (in Serbian).

[3] Hajdin, N.: *The Theory of Surface Mounts*, Faculty of Civil Engineering, University of Belgrade, Belgrade, 1984, (in Serbian).

[4] Haßler, M. and Schweizerhof, K.: On the stability analysis of thin walled shell structures containing gas or fluid, in: *Book of Abstracts of the III European Conference on Computational Mechanics*, 05-08.06.2006, Lisbon, Portugal, p. 695.

[5] Vanlaere, W., Van Impe, R., Lagae, G., Katnam, K.B. and De Beule, M.: On the imperfections of cylindrical shells on local supports, in: Liu, G.R., Tan, V.B.C. and Han, X. (Eds.): *Computational Methods*, Springer, Dordrecht, pp. 1767-1771, 2006.

[6] Guggenberger, W.: Elastic stability and imperfection sensitivity of axially loaded cylindrical shells on narrow supports, Computational Mechanics, Vol. 37, No. 6, pp. 537-550, 2006.

[7] Zenkour, A.M.: Stress analysis of axisymmetric shear deformable cross-ply laminated circular cylindrical shells, Journal of Engineering Mathematics, Vol. 40, No. 4, pp. 315-332, 2001.

[8] Fryer, D.M. and Harvey, J.F.: *High Pressure Vessels*, Chapman & Hal, New York, 1998.

[9] Baličević, P., Kozak, D. and Mrčela, T.: Strength of pressure vessels with ellipsoidal heads, Strojniški vestnik – Journal of Mechanical Engineering, Vol. 54, No. 10, pp. 685-692, 2008.

[10] Baličević, P., Kozak, D. and Kraljević, D.: Analytical and numerical solutions of internal forces by cylindrical pressure vessel with semi-elliptical heads, in: *Proceedings of the 1st International Congress of Serbian Society of Mechanics*, 10-13.04.2007, Kopaonik, Serbia, pp. 1-6.

[11] Petrović, R., Kojić, M. and Đorđević, D.: *Design of the Tanks for Storage and Transport of Fluids*, Faculty of Mechanical Engineering, University of Kragujevac, Kraljevo, 2005, (in Serbian).

[12] Bathe, K.-J. and Ho, L.-W.: A simple and effective element for analysis of general shell structures, Computers & Structures, Vol. 13, No. 5-6, pp. 673-681, 1981.

[13] Dhatt, G. and Touzot, G.: *The Finite Element Method Displayed*, John Wiley & Sons, Hoboken, 1984.

[14] Strang, G. and Fix, G.J.: *An Analysis of the Finite Elements Method*, Prentice-Hall, Upper Saddle River, 1973.

[15] Segerlind, L.J.: *Applied Finite Element Analysis*, John Wiley & Sons, Hoboken, 1975.

[16] Kojić, M., Slavković, R. and Živković, M.: *Finite Element Method I*, Faculty of Mechanical Engineering, University of Kragujevac, Kragujevac, 1998, (in Serbian).

[17] Kojić, M. and Micić, Ž.: Comparative analysis of the finite element plates and shells in solving linear and geometric nonlinear problems, in: *Proceedings of the Scientific Conference PPPR*, 22-23.11.1982, Stubičke Toplice, Croatia, pp. 269-274, (in Serbian).

[18] Micić, Ž. and Kojić, M.: Contribution of analysis using finite element plate and shell, in: *Proceedings of the VIII International Symposium – PPPR*, 15-16.10.1986, Zagreb, Croatia, pp. 259-264, (in Serbian).

[19] Ashwell, D.G. and Sabir, A.B.: A new cylindrical shell finite element based on simple independent strain functions, International Journal of Mechanical Sciences, Vol. 14, No. 3, pp. 171-183, 1972.

NOMENCLATURE

$w(x,y)$ deflection of the tank shell

Z	load symmetrically in relation to the axis of the cylinder
E	modulus of elasticity
r	radius of the tank
$w_p(x)$	particular integral of equation (1)
C_1, C_2, C_3, C_4	constants of integration
g	acceleration of gravity
h	height of the tank
h_1	height of segment "1"
h_2	height of segment "2"
M_x	bending moment in the direction x
M_φ	moment in the circular direction
Q_x	transverse force in the direction x

Greek symbols

β	coefficient
ν	Poisson's ratio
δ	thickness of the tank shell plate
δ_1	thickness of segment "1"
δ_2	thickness of segment "2"
ρ	fluid density
σ_x	bending stress in the direction x
σ_φ	stress in the circular direction
$\tau_{\max}$	maximum shear stress
σ_e	equivalent stress
σ_{doz}	allowed stress

ИДЕНТИФИКАЦИЈА ДЕФОРМАЦИЈСКО НАПОНСКОГ СТАЊА ЦИЛИНДРИЧНОГ РЕЗЕРВОАРА СА ЗИДОВИМА ПРОМЕНЉИВЕ ДЕБЉИНЕ

Мирко Ђелошевић, Драган Петровић, Милан Бижић

У овом раду је извршена деформацијско-напонска анализа омотача цилиндричног резервоара, израђеног из два сегмента различитих дебљина, оптерећеног хидростатичким притиском воде. Формирани су физички и математички модели меродавни за анализу угиба и напона омотача у функцији од хидростатичког притиска. Одређене су функције расподеле угиба, трансверзалних сила и одговарајућих момената омотача односно сегмената резервоара, као и напона. Идентификован је међусобан утицај појединог сегмента резервоара на остале, у зависности од дужине и дебљине лима примењених сегмената, чиме је створена могућност оптималног пројектовања резервоара симетрично оптерећених у односу на осу. Добијени резултати аналитичким поступком су у сагласности са резултатима МКЕ, дијаграми расподеле угиба, момената, трансверзалних сила и напона су идентични, док максимално одступање тих величина не прелази 5 %.